Journal of Nuclear Materials 390–391 (2009) 168–171

Contents lists available at ScienceDirect

Journal of Nuclear Materials

journal homepage: www.elsevier.com/locate/jnucmat

Numerical analysis of incident angle of heavy metal impurity to plasma facing components by IMPGYRO

K. Hoshino [a,*], M. Toma [b], M. Furubayashi [b], A. Hatayama [b], K. Inai [c], K. Ohya [c]

[a] Naka Fusion Institute, Japan Atomic Energy Agency, 801-1 Mukouyama, Naka-shi, Ibaraki-ken 311-0193, Japan
[b] Faculty of Science and Technology, Keio University, Kanagawa 223-8522, Japan
[c] Institute of Technology and Science, The University of Tokushima, Tokushima 770-8501, Japan

ARTICLE INFO

PACS:
52.25.Fi
52.25.Vy
52.40.Hf
52.65.Pp

ABSTRACT

The self-sputtering and reflection yields are important for a prediction of the tungsten impurity content penetrating into the main plasma in future fusion reactors. The self-sputtering and reflection yields greatly depend on the incident angle of impurities to plasma facing components. The IMPGYRO code is applied to the analysis of angle distribution of incident impurities, effects of the sheath on the incident angle and energy, and the resultant sputtering and reflection yield. The incident angle distribution is divided into several peaks by the sheath effect. Each peak corresponds to the peak for each charge state. In high temperature condition for the divertor plasma, the sputtering yield increases mainly due to the change of incident angle by the sheath. In low temperature condition, the effects of the sheath on the sputtering yield and the reflection yield are small because of low incident energy and large incident angle.

1. Introduction

Recently, tungsten has been paid attention as a divertor plate material due to a low sputtering yield, low tritium retention, etc. Furthermore, in a detached divertor operation, the physical sputtering by fuel ions is expected to largely decrease. However, the physical sputtering still remains due to the impurities (C, He, Ar, etc.) or the high energy CX (charge-exchange) neutrals produced inside the main plasma. In addition, the physical sputtering due to the self-sputtering might be significantly large. The atomic number and charge number of tungsten are so high that radiation cooling of the main plasma might occur even if a small amount of tungsten enters to the main plasma.

The proper evaluation of the multiplication factor on the divertor, i.e., the sum of the self-sputtering yield and the reflection yield is important for prediction of the impurity content penetrating into the main plasma. Fig. 1 shows an incident angle dependence of a self-sputtering yield and a reflection yield calculated by the erosion and deposition based on dynamic model (EDDY) code [1]. The self-sputtering yield and reflection yield greatly depend on an incident angle of impurities. Therefore proper calculation of an incident angle is needed for evaluation of the multiplication factor on the divertor.

In this study, the IMPGYRO code [2–5] is applied to the analysis of the incident angle of tungsten impurities to the plasma facing component such as the divertor plate. The effect of the sheath on the incident angle and energy, and the resultant sputtering and reflection yields are discussed.

2. Simulation model

The IMPGYRO code [2–5] is a Monte-Carlo transport code to understand a transport process of heavy metal impurity in the edge plasma and to predict the impurity content penetrating into the main plasma in the future fusion reactors. The code includes important processes of heavy metal impurities, such as Larmor gyration, Coulomb collisions [6], the thermal force [7] and the multi-step ionization/recombination processes [8]. In order to take into account Larmor gyration, the three dimensional equation of motion is directly solved in a realistic Tokamak geometry. The code is being developed at Keio University as a host institute and has been optimized on a parallel computer recently. In addition, some numerical algorithm and physics model, especially surface interaction model have been improved from previous version of the IMPGYRO code [4]. More specifically, coupling to the EDDY code [1,5] and the implementation of the sheath model have been done.

The simple sheath model is implemented under following assumptions: (1) the tungsten density is much smaller than background plasma. Therefore, the formation of the sheath does not depend on the tungsten impurity. (2) A sheath width is much narrow compared with a Larmor radius of tungsten. Therefore a gyro-motion in a sheath region can be neglected. The incident energy at the wall is given by following energy conservation law:

* Corresponding author.
E-mail address: hoshino.kazuo@jaea.go.jp (K. Hoshino).

0022-3115/$ - see front matter © 2009 Elsevier B.V. All rights reserved.
doi:10.1016/j.jnucmat.2009.01.159

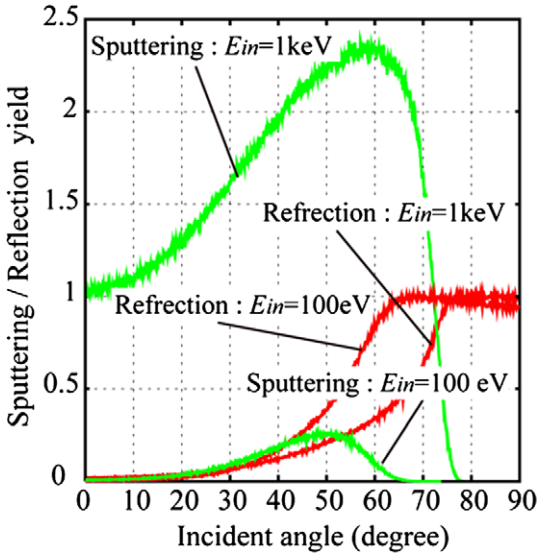

Fig. 1. The incident angle dependence of the self-sputtering yield and the reflection yield calculated by the EDDY code [1]. Here, the incident angle is measured from the wall normal. Both of the target atom and the incident atom are tungsten. Two cases for typical incident energy are plotted.

$$E_{\mathrm{wall}} = E_{\mathrm{se}} + Ze\phi, \tag{1}$$

where E is a kinetic energy of an incident particle, Z is a charge state. Subscript 'wall' and 'se' mean 'at the wall' and 'at the sheath entrance', respectively. The sheath potential drop ϕ is estimated by a simple formula $\phi = 3kT_e/e$, where T_e is the electron temperature at the incident point. The incident angle at the wall θ_{wall} is calculated by following expression:

$$\theta_{\mathrm{wall}} = \arccos(v_{\perp,\mathrm{wall}}/v), \tag{2}$$

where v is absolute value of the incident velocity. The velocity normal to the wall $v_{\perp,\mathrm{wall}}$ is evaluated from the energy conservation law Eq. (1):

$$v_{\perp,\mathrm{wall}} = \sqrt{v_{\perp,\mathrm{se}}^2 + \frac{2}{m_w} Ze\phi}, \tag{3}$$

where m_W is mass of tungsten ions.

The background plasma profile is calculated by the B2.5-EIRENE code [9], and fixed during the calculation by the IMPGYRO code. Two background plasma profiles are used in the analysis. In the calculation of the background plasmas by the B2.5-EIRENE code, the boundary condition for the bulk ion density at the core interface boundary ($r/a = 0.95$) is fixed to $n_D = 1.5 \times 10^{19}\ \mathrm{m}^{-3}$ for the case A and $n_D = 2.8 \times 10^{19}\ \mathrm{m}^{-3}$ for the case B. The total input power is set to be 2.5 MW in the both cases. Other simulation conditions are the same as the case without drift effects in Refs. [10,11]. Fig. 2 shows the spatial profiles of the electron density and temperature. Case B is low temperature condition, i.e., the electron temperature

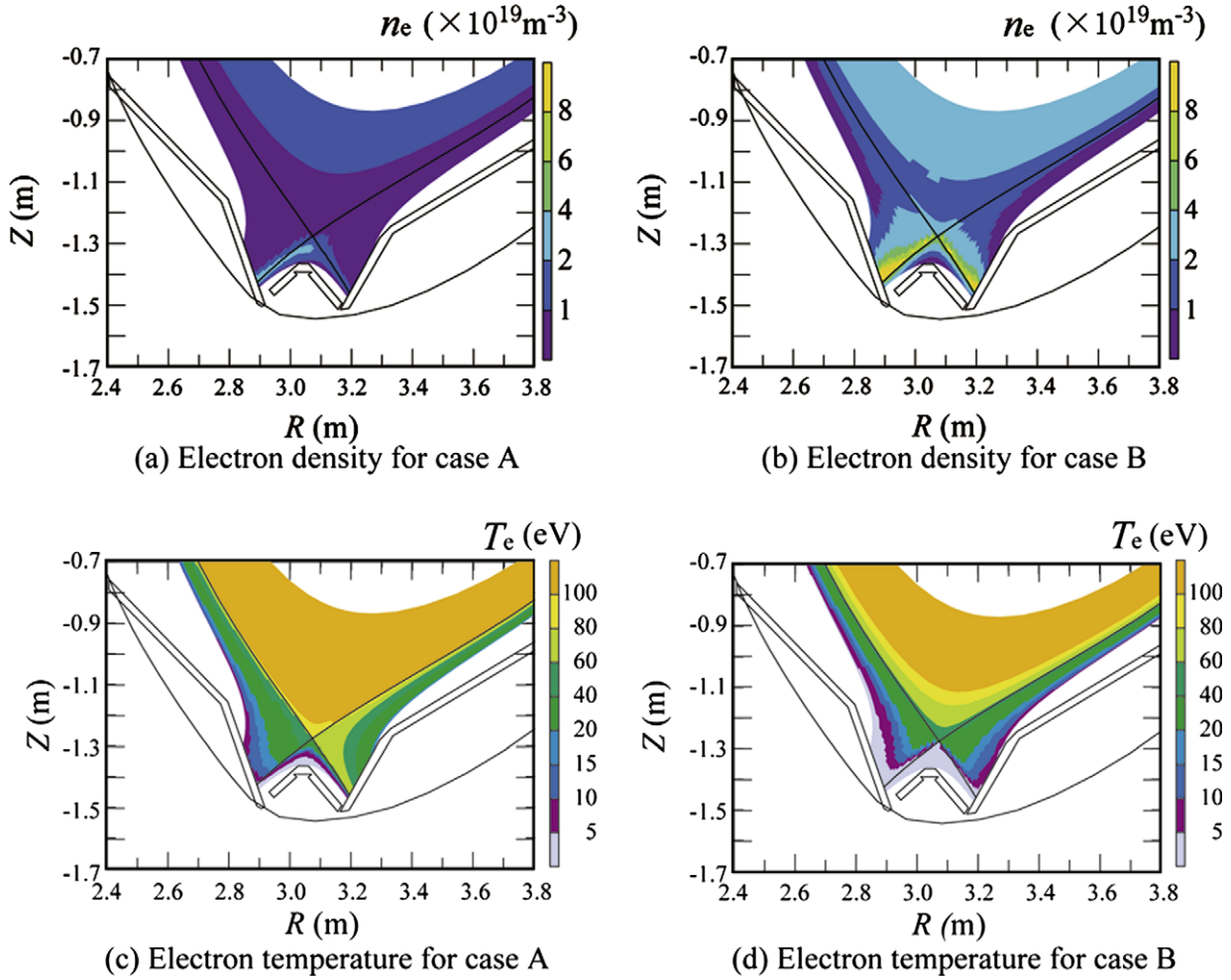

Fig. 2. Background plasma profiles calculated by the B2.5-EIRENE code.

in front of the divertor is less than 5 eV, while case A is high temperature condition.

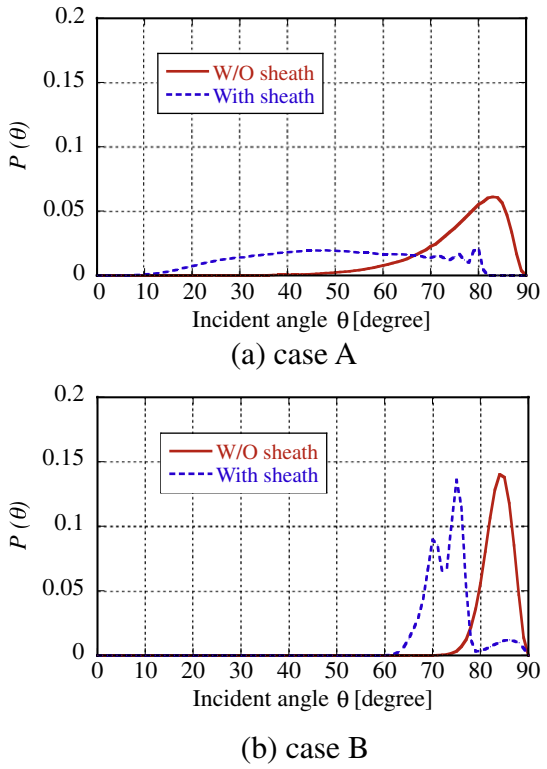

Fig. 3. The angle distribution of the incident particles without and with the sheath effect. Vertical axis $P(\theta)$ is defined as $P(\theta)$ = (number of incident particles with θ)/(total number of incident particles).

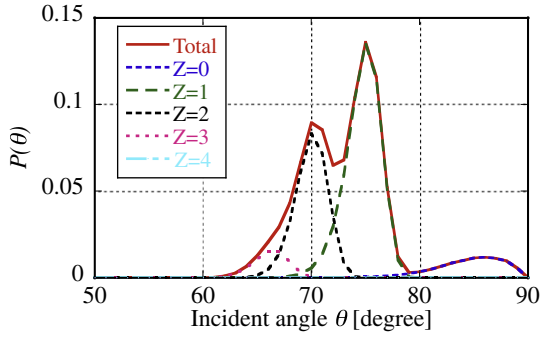

Fig. 4. The incident angle distribution for charge state $Z = 0+ \sim 4+$ on the outer divertor of case B.

In the present analysis, relatively simple setup has been adopted, especially for the first generation of the tungsten impurities: 10^6 test particles are uniformly launched from the plasma wetted area on the divertor plate as a neutral tungsten particle with monotonic energy of 10 eV.

3. Results

Fig. 3 shows the distribution of the incident angle to the outer divertor plate. The profile without the sheath effect is widely distributed around the incident angle of a magnetic line of force (about 87°).

Due to the sheath acceleration, the profile of incident angle shifts toward smaller angle. Especially in the case B, the profile is divided into several peaks. This separation of the peak is caused by the difference of the charge state of the incident ions. The incident angle distribution for each charge state on the outer divertor of case B is shown in Fig. 4. The peaks of the incident angle distribution for each charge state are clearly separated because the acceleration of the incident impurity ions depends on each charge state. Of course, because the sheath does not affect on the neutral particles, the profile of the impurity neutrals ($Z = 0$) does not shift.

Table 1 shows the sputtering and reflection yields with and without the sheath effects. As for the case with the sheath effect, following three cases are shown: (1) angle – only a change of the incident angle by the sheath is considered, i.e., the sputtering and reflection yields are calculated from θ_{wall} and E_{se}, (2) energy – the sputtering and reflection yields are calculated from θ_{se} and E_{wall}, (3) both – the change both of the incident angle and energy is considered.

In case A – 'W/O sheath', the reflection is dominant because of the large incident angle as shown in Fig. 3(a). Due to a change of the incident angle, the sputtering yield increases 10 times larger, while the reflection yield decreases. On the other hand, the increase of sputtering yield by the change of the incident energy is about four times. The total yield, i.e., the multiplication factor on the divertor becomes more than 2 mainly due to the effect of the sheath on the incident angle, and the sputtering becomes dominant. In the case B, the reflection is dominant in all cases because of the low incident energy and relatively large incident angle. As shown in Fig. 1, the reflection yield is not sensitive around horizontal incidence. Therefore, the significant effect of the sheath on the multiplication factor cannot be seen in case B.

4. Summary

The IMPGYRO code is improved to take into account a sheath model. In this paper, the effect of the sheath on the incident angle, and the resultant self-sputtering and reflection yields were discussed.

Incident angle is widely distributed around the incident angle of a magnetic line of force. Due to a sheath effect, the peak of incident angle shifts toward smaller angle. Particularly, in the case B, the

Table 1
The sputtering yield, reflection yield and total yield (multiplication factor) on the outer divertor plate. The case with the sheath effect is separated into following three cases: (1) the change only of the incident angle by the sheath, (2) the change only of the incident energy by the sheath, (3) the change both of the incident angle and energy.

	Case A			Case B		
	Sputtering	Reflection	Total	Sputtering	Reflection	Total
W/O sheath	0.156	0.929	1.085	0.000	0.975	0.975
With sheath						
(1) Angle	1.565	0.324	1.889	0.005	0.983	0.987
(2) Energy	0.683	0.859	1.542	0.000	0.978	0.977
(3) Both	2.349	0.301	2.651	0.008	0.982	0.990

peak for the case with the sheath effect is divided into several peaks. Each peak corresponds to the peak of incident angle distribution for each charge state.

In case A, i.e., high temperature condition for the divertor plasma, the self-sputtering yield increases mainly due to the change of the incident angle by the sheath effect. In case B, i.e., the low temperature condition, the significant effect of the sheath on the multiplication factor cannot be seen.

In order to predict the impurity content penetrating into the main plasma, the following further improvements of the code will be required: (1) detail modeling of the initial generation, (2) expansion of the calculation domain to further deep into the core region, the wall and the doom, (3) iterative coupling with a background plasma simulation code, and (4) quantitative comparisons with the experiments and other impurity transport codes to validate the physics models.

Acknowledgement

This study is partially supported by a Grant-in-Aid for Scientific Research of the Japan Society for the Promotion of Science.

References

[1] K. Ohya et al., Phys. Scr. T124 (2006) 70.
[2] I. Hyodo et al., J. Nucl. Mater. 313–316 (2003) 1183.
[3] A. Fukano et al., J. Nucl. Mater. 363–365 (2007) 211.
[4] K. Hoshino et al., Contribution Plasma Phys. 48 (2008) 280.
[5] M. Toma et al., J. Nucl. Mater. 390–391 (2009) 207.
[6] T. Takizuka et al., J. Comp. Phys. 25 (1977) 205.
[7] J. Neuhauser et al., Nucl. Fus. 24 (1984) 39.
[8] A. Suzuki et al., J. Comp. Physiol. 131 (1997) 193.
[9] R. Schneider et al., Contribution Plasma Phys. 46 (2006) 3.
[10] K. Hoshino et al., Contribution Plasma Phys. 46 (2006) 591.
[11] K. Hoshino et al., J. Nucl. Mater. 337–339 (2005) 276.